Supplementary Information (SI) for Journal of Materials Chemistry A.

Electronic supplementary information

Direct utilization of light energy to promote the power density of zinc-air batteries using $Co_3O_4@Cu_xO$ air photocathodes with porous octahedral superstructures

Yuhao Zhong,[a] *Jing Xie,*[ab] *Ruitong Xu,*[a] *Xiaobo Feng,*[ac] *and Ting Zhu*[ac]*

[a] School of Physics and Electronic Information, Yunnan Normal University, 768 Juxian Street, Kunming 650500, Yunnan, China.

[b] School of Materials Science and Engineering, Central South University, 932 Lushan Road South, Changsha 410083, Hunan, China.

[c] Yunnan Key Laboratory of Optoelectronic Information Technology, School of Physics and Electronic Information, Yunnan Normal University, Kunming 650500, China.

*Email: zhut0002@ynnu.edu.cn (T. Zhu)

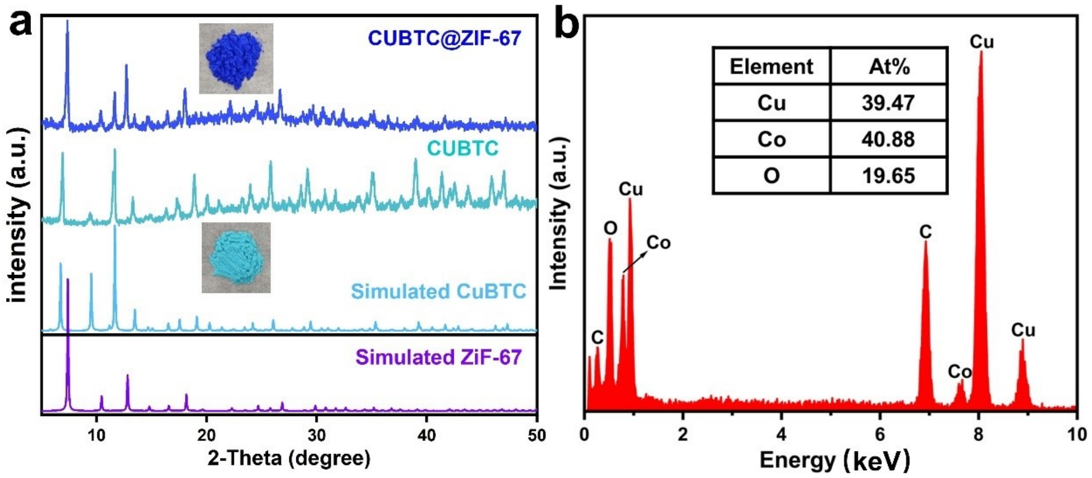

Fig. S1. XRD (a) and EDX (b) patterns of CuBTC (a) and ZIF67@CuBTC (a and b).

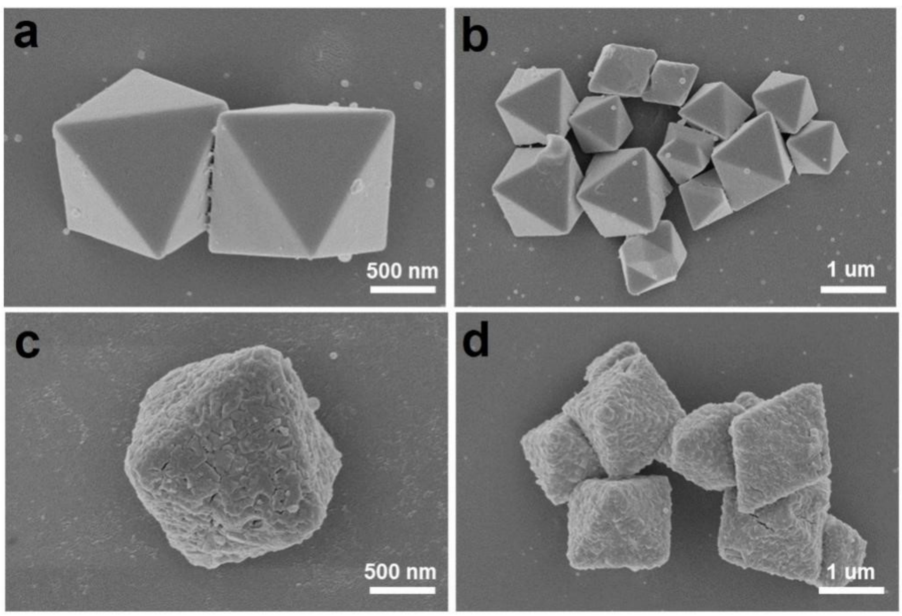

Fig. S2. SEM images of CuBTC (a and b) and ZIF67@CuBTC (c and d).

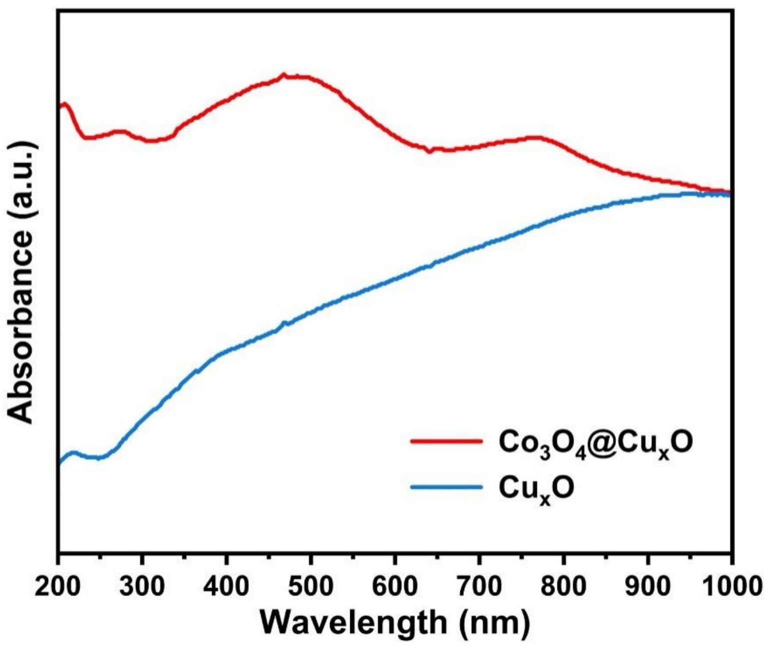

Fig. S3. UV-Vis-NIR spectra of the Cu_xO and $Co_3O_4@Cu_xO$ samples.

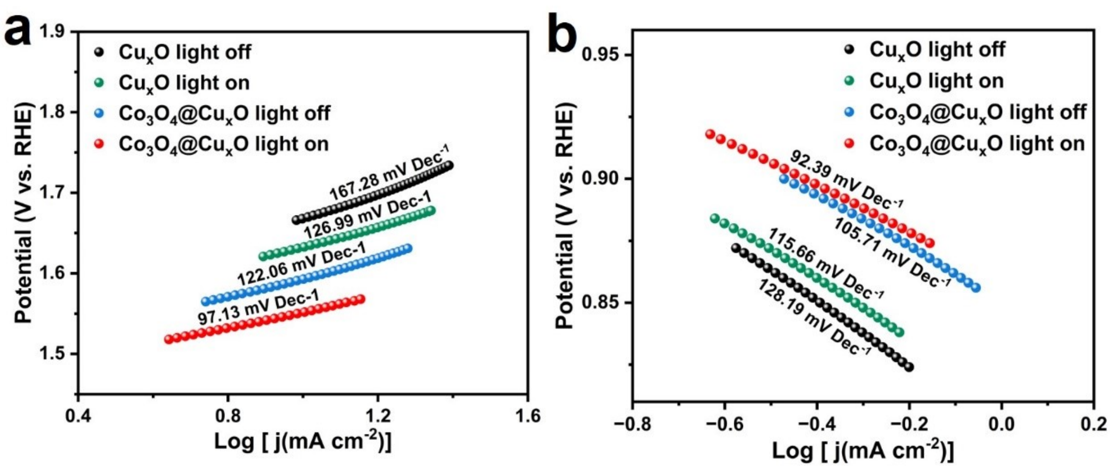

Fig. S4. Tafel plots of OER (a) and ORR (b) for the Cu_xO and $Co_3O_4@Cu_xO$ samples obtained under light on and off conditions, respectively.

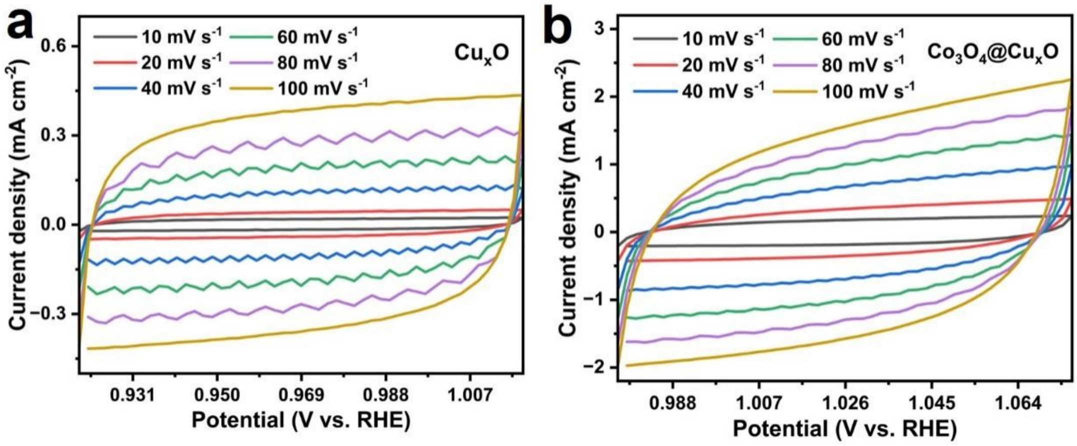

Fig. S5. CV curves collected from the non-Faradaic regions of the Cu_xO (a) and $Co_3O_4@Cu_xO$ (b) samples, respectively.

.

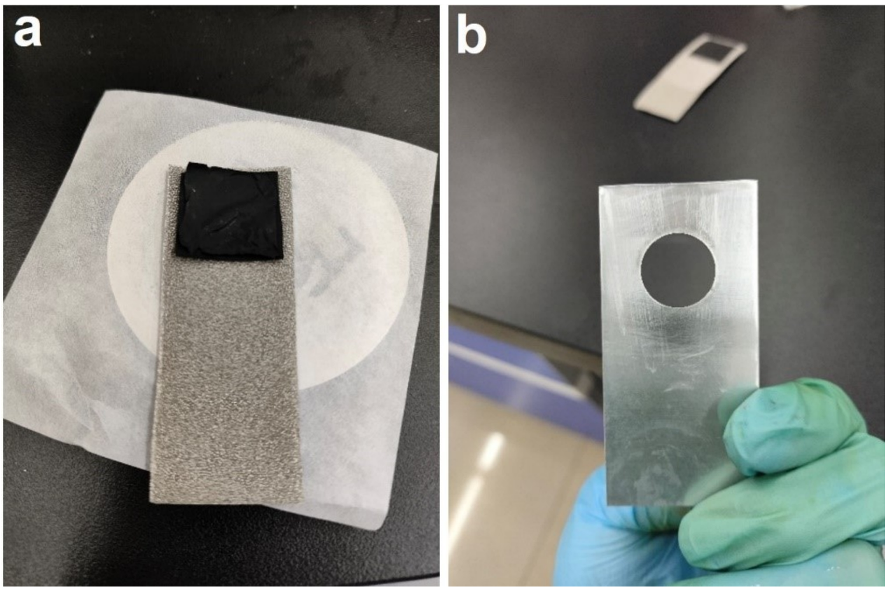

Fig. S6. Optical images of the building components of a ZAB cell: the air cathode (a, composed of water-proof membrane, nickel foam, and $Co_3O_4@Cu_xO$/PTFE/ acetylene black film), and the Zn foil anode (b, with a punched hole for light passing through).

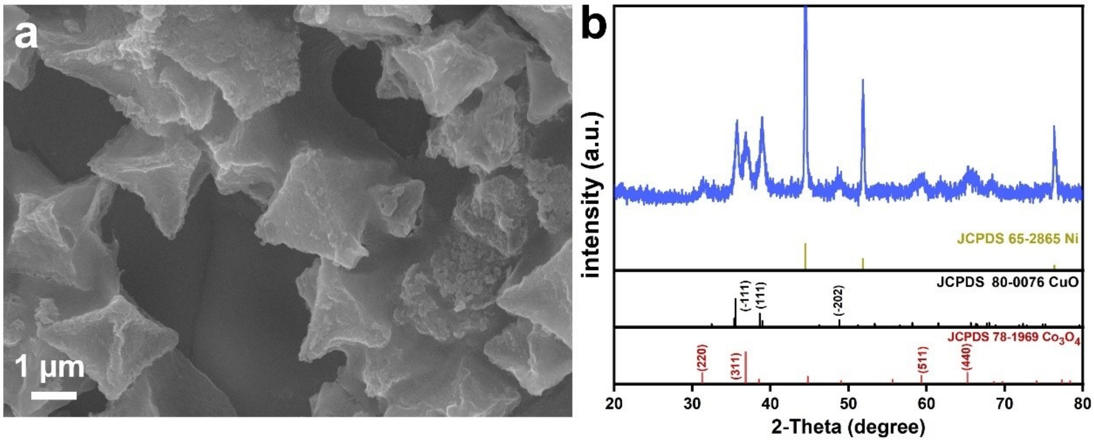

Fig. S7. The SEM image (a) and XRD pattern (b) of the Co_3O_4@Cu_xO sample after cycling test.

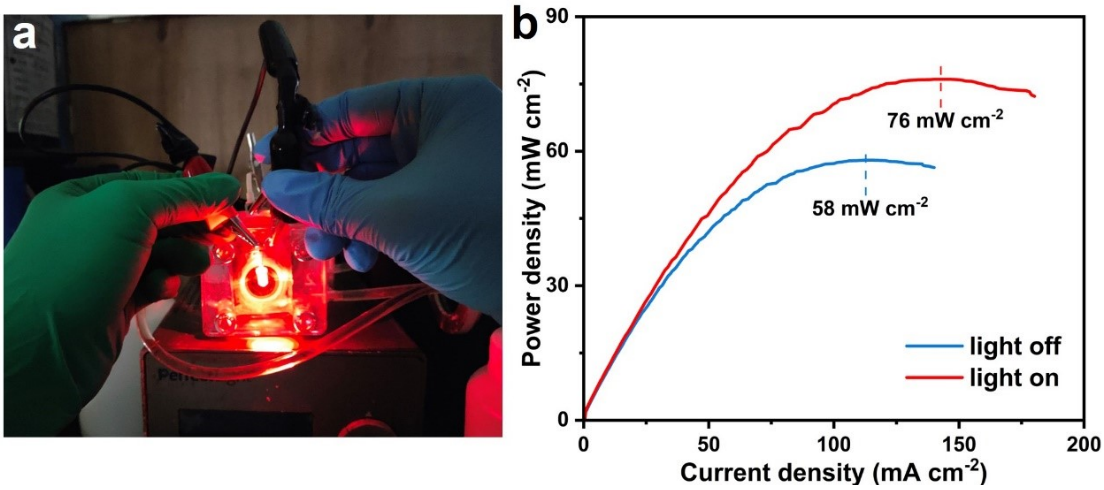

Fig. S8. A demonstration of a red LED lighted up by two connected ZAB cells (a), and power densities of the Co_3O_4@Cu_xO-based ZABs obtained with light on and off conditions, respectively. The power densities were calculated by the discharge current densities shown in Fig. 4c.

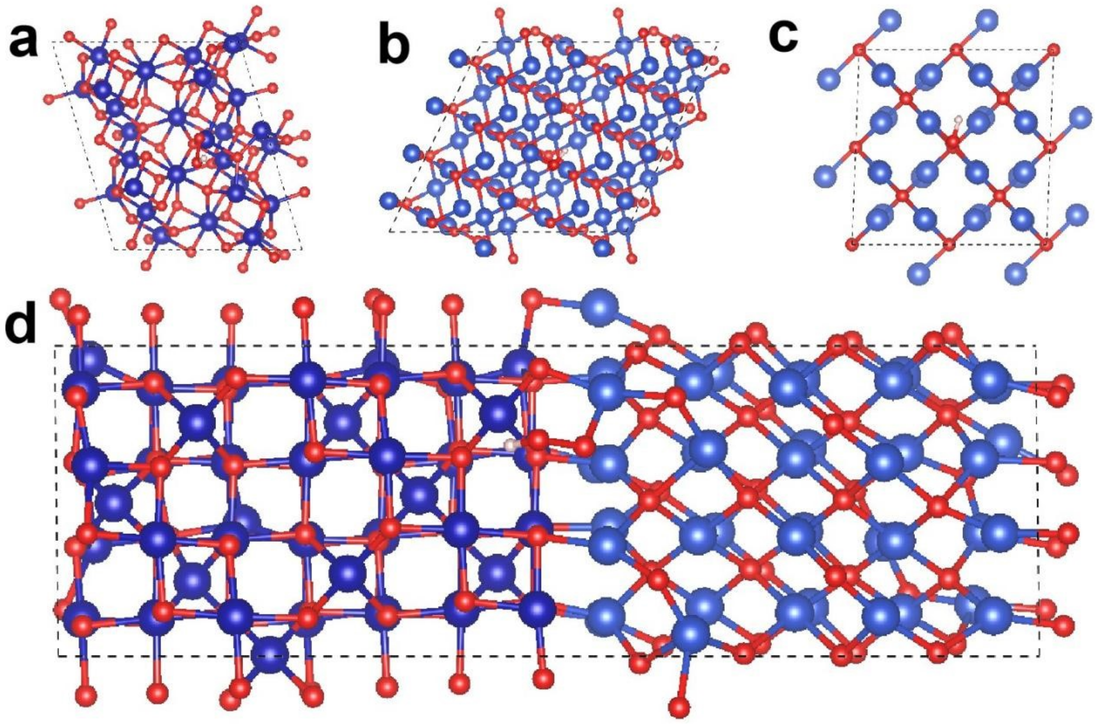

Fig. S9. Optimized atomic configurations of OOH* adsorbed on Co_3O_4(311) (a), CuO(-111) (b), Cu_2O(200) (c), and Co_3O_4@Cu_xO heterojunction(d), respectively.

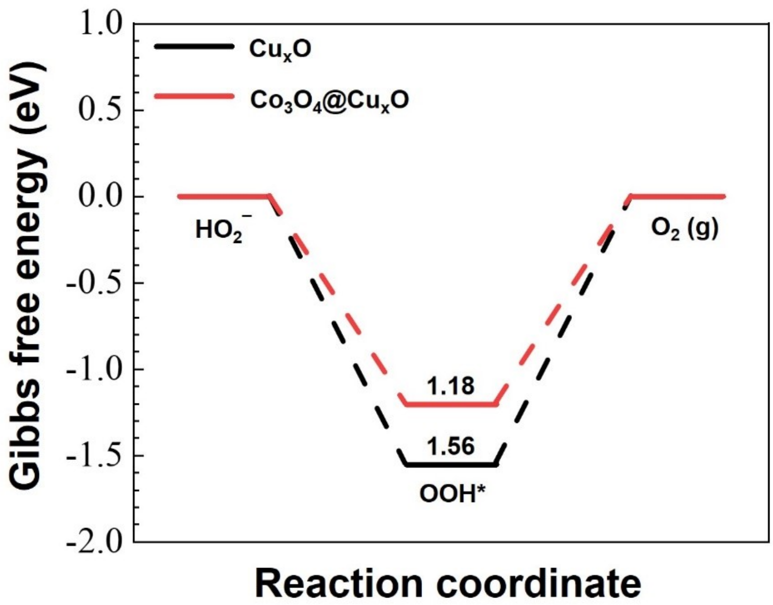

Fig. S10. Free energy diagrams at 0.68 V of OER processes on Cu_xO and Co_3O_4@Cu_xO, respectively.

Table S1. A comparison of the air cathode materials for ZABs with and without light enhancements.

Type	Cathode materials	Charge voltage /V		Current density /mA cm^{-2}	Light enhancement /%	Cycling /h	Capacity / mA h g^{-1}	Power density /mW cm^{-2}	Ref.
		Dark	Light						
Photo-enhanced ZABs	**Co_3O_4@Cu_xO**	**1.837**	**1.748**	**0.1**	**31**	**160**	**759.12**	**76**	**This work**
	α-Fe_2O_3	1.97	1.43	0.1	27.4	/	598.7	75.49	[1]
	$BiVO_4$	1.96	1.20	0.1	38.8	/	538.5	69.24	[1]
	Co_3O_4	2.10	2.00	2	5.00	70	769	/	[2]
	$NiCo_2S_4$	1.97	1.92	2	2.54	12	734	/	[3]
	Ni_2P_5@NCNT	1.94	1.90	10	2.10	8.8	640	190	[4]
	PTTH	2.08	1.92	0.1	7.69	316	/	/	[5]
	CuO/ZnO	2.27	1.5	0.05	33.7	3	333.5	34.01	[6]
	TiO_2@In_2Se_3@Ag_3PO_4	/	0.64	0.1	/	210	/	13.1/	[7]
	g-C_3N_4-CuZIF-67	2.01	1.94	2	3.5	20	781.7	/	[8]
Conventional ZABs	Co_2FeO_4@NCNTs	2.32	/	50	/	100	/	90.68	[9]
	Co_3O_{4-x}@C	2.07	/	10	/	358	/	54.5	[10]
	Co@Co_3O_4@NAC	2.10	/	5	/	36	721	164	[11]
	Fe_3C/Fe_2O_3@NGNs	2.11	/	10	/	40	722	139.8	[12]
	FeN_x/C	2.08	/	5	/	84	/	36	[13]

[1] Liu X, Yuan Y, Liu J, et al. Utilizing solar energy to improve the oxygen evolution reaction kinetics in zinc-air battery[J]. Nat Commun, 2019, 10(1): 4767.

[2] Tomon C, Sarawutanukul S, Duangdangchote S, et al. Photoactive Zn-air batteries using spinel-type cobalt oxide as a bifunctional photocatalyst at the air cathode[J]. Chem Commun (Camb), 2019, 55(42): 5855-5858.

[3] Sarawutanukul S, Tomon C, Duangdangchote S, et al. Rechargeable Photoactive Zn-Air Batteries Using $NiCo_2S_4$ as an Efficient Bifunctional Photocatalyst towards OER/ORR at the Cathode[J]. Batteries & Supercaps, 2020, 3(6): 541-547.

[4] Lv J, Abbas S C, Huang Y, et al. A photo-responsive bifunctional electrocatalyst for oxygen

reduction and evolution reactions[J]. Nano Energy, 2018, 43: 130-137.
[5] Zhu D, Zhao Q, Fan G, et al. Photoinduced Oxygen Reduction Reaction Boosts the Output Voltage of a Zinc-Air Battery[J]. Angew Chem Int Ed Engl, 2019, 58(36): 12460-12464.
[6] Bu D, Batmunkh M, Zhang Y, et al. Rechargeable sunlight-promoted Zn-air battery constructed by bifunctional oxygen photoelectrodes: Energy-band switching between ZnO/Cu_2O and ZnO/CuO in charge-discharge cycles[J]. Chemical Engineering Journal, 2022, 433: 133559.
[7] Feng H, Zhang C, Liu Z, et al. A light-activated $TiO_2@In_2Se_3@Ag_3PO_4$ cathode for high-performance Zn-Air batteries[J]. Chemical Engineering Journal, 2022, 434: 134650.
[8] Ren R, Liu G, Kim J Y, et al. Photoactive $g\text{-}C_3N_4$/CuZIF-67 bifunctional electrocatalyst with staggered p-n heterojunction for rechargeable Zn-air batteries[J]. Applied Catalysis B: Environmental, 2022, 306: 121096.
[9] Wang X T, Ouyang T, Wang L, et al. Redox-Inert Fe(3+) Ions in Octahedral Sites of Co-Fe Spinel Oxides with Enhanced Oxygen Catalytic Activity for Rechargeable Zinc-Air Batteries[J]. Angew Chem Int Ed Engl, 2019, 58(38): 13291-13296.
[10] Chen D, Pan L, Pei P, et al. Carbon-coated oxygen vacancies-rich Co_3O_4 nanoarrays grow on nickel foam as efficient bifunctional electrocatalysts for rechargeable zinc-air batteries[J]. Energy, 2021, 224: 120142.
[11] Zhong X, Yi W, Qu Y, et al. Co single-atom anchored on Co_3O_4 and nitrogen-doped active carbon toward bifunctional catalyst for zinc-air batteries[J]. Applied Catalysis B: Environmental, 2020, 260: 118188.
[12] Tian Y, Xu L, Qian J, et al. Fe_3C/Fe_2O_3 heterostructure embedded in N-doped graphene as a bifunctional catalyst for quasi-solid-state zinc–air batteries[J]. Carbon, 2019, 146: 763-771.
[13] Han S, Hu X, Wang J, et al. Novel Route to Fe-Based Cathode as an Efficient Bifunctional Catalysts for Rechargeable Zn-Air Battery[J]. Advanced Energy Materials, 2018, 8(22): 1800955.